ChemComm

COMMUNICATION

View Article Online
View Journal | View Issue

Cite this: *Chem. Commun.*, 2018, **54**, 7959

Received 24th May 2018,
Accepted 22nd June 2018

DOI: 10.1039/c8cc04127j

rsc.li/chemcomm

Orthogonal reactivity of Ni(I)/Pd(0) dual catalysts for Ullmann C–C cross-coupling: theoretical insight†

Bo Zhu, [a] Li-Kai Yan, [a] Li-Shuang Yao,[b] Hang Ren,[a] Run-Han Li,[a] Wei Guan *[ab] and Zhong-Min Su *[a]

Dual catalysis has become a desirable alternative because of the synergetic effect of two distinct catalysts, but little is known about the mechanism of dual catalysis and its effect on the high reactivity and selectivity. Here, a novel Ullmann C–C cross-coupling of bromobenzene and 4-methoxyphenyltriflate *via* nickel/palladium dual catalysis has been investigated using density functional theory. The orthogonal reactivity of Ni^{I}/Pd^{0} combination is the precondition and foundation of achieving such a Ullmann cross-coupling reaction. In the present dual catalysis, the Ni^{I} complex acts as the primary catalyst, while the Pd^{0} catalyst plays a decisive role in the cross-selectivity.

Transition metal catalyzed C–C cross-couplings have revolutionized chemical synthesis to generate versatile organic building blocks for diverse natural products and fine chemicals.[1,2] In addition to the cross-couplings between nucleophiles and electrophiles such as Heck, Negishi, Suzuki couplings and so on,[3] Ullmann coupling without organometallic reagents has set the stage for reductive cross-electrophile couplings since Ullmann and Goldberg first reported it more than a century ago.[4] Ullmann coupling *via* dual catalysis has the characteristics of operational simplicity, sustainability and low cost, but low selectivity and yields of the desired product limit the further development of this potentially powerful strategy to a great extent because of the competition for oxidative addition of both electrophiles to the catalyst.[5] Recently, Weix and co-workers successfully developed an unprecedented highly selective Ullmann C–C cross-coupling of bromobenzene (**Ph-Br**) and 4-methoxyphenyltriflate (**Ar-OTf**) utilizing Ni/Pd dual catalysis.[6] As shown in Scheme 1, in the presence of Zn dust, Ni/Pd dual catalysts provided high cross-selectivity and yields of C–C cross-coupling products. By contrast, the homo-coupling product biphenyl was predominantly afforded when the Ni catalyst was allowed to react independently with the two substrates. Obviously, the orthogonal reactivity between Ni/Pd dual catalysts to the two aryl electrophiles is a key requirement for constructing selectively the C–C bond *via* cross-coupling. Thus, it is crucial to correctly reveal the corresponding Ni/Pd active catalysts and the origin of orthogonal reactivity to substrates between dual catalysts. Furthermore, a clear understanding of how Ni/Pd dual catalysis improves the cross-selectivity will inspire the chemists to develop versatile reductive cross-electrophile coupling reactions. However, the specific mechanism of Ni/Pd dual catalysis still remains ambiguous regarding many mechanistic subtleties and multiple oxidation states of Ni and Pd dual catalysts in the reaction process. Theoretical calculations have become essential to provide meaningful information of structures and properties of molecules as well as mechanisms and selectivities of reactions.[7]

Here, we theoretically investigated all the reaction processes involved in Scheme 1, where **Ph-Br** and **Ar-OTf** were employed as substrates, while 2,2-bipyridine (bpy) and 1,3-bis(diphenylphosphino)propane (dppp) were employed as ligands, as in the experiments.[6] Geometry optimizations, intrinsic reaction coordinate calculations, and vibrational frequency calculations were performed at the CPCM[8](DMF)/(U)M06[9]/[6-31G(d)/SDD(Ni,Pd)] level to determine the potential energy surfaces. The spin-unrestricted (broken-symmetry) approach was used in the optimizations involving diradical structures. The translational entropy correction was included to treat the standard state.[10] Electronic energies were evaluated at the CPCM (DMF)/(U)M06/[6-311++G(d,p)/SDD(Ni,Pd)] level. These calculations were carried out with the Gaussian 09 program[11] (see the ESI† for methods).

To realize the present Ullmann C–C cross-coupling, Ni/Pd dual catalysts must provide the orthogonal reactivity to **Ph-Br** and **Ar-OTf** (Scheme 1). Note that Zn dust as a reducing agent might enrich the oxidation states of Ni and Pd involving Ni(I), Ni(0), and Pd(0). Therefore, we have fully evaluated the chemoselectivity of the

[a] *Faculty of Chemistry, National & Local United Engineering Lab for Power Battery, Key Laboratory of Polyoxometalate Science of Ministry of Education, Northeast Normal University, Changchun 130024, P. R. China. E-mail: guanw580@nenu.edu.cn, zmsu@nenu.edu.cn*

[b] *State Key Laboratory of Applied Optics, Changchun Institute of Optics, Fine Mechanics and Physics, Chinese Academy of Sciences, Changchun 130033, P. R. China*

† Electronic supplementary information (ESI) available: Methods, complete ref. 11, Fig. S1–S8, and Cartesian coordinates of optimized structures in this work. See DOI: 10.1039/c8cc04127j

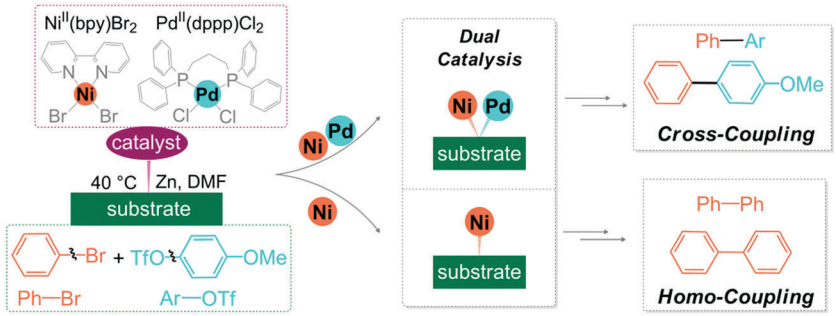

Scheme 1 The Ullmann reaction of **Ph-Br** with **Ar-OTf** catalyzed by $Ni^{II}(bpy)Br_2$/$Pd^{II}(dppp)Cl_2$ and $Ni^{II}(bpy)Br_2$, respectively.[6]

oxidative additions of **Ph-Br** and **Ar-OTf** to Ni and Pd with different oxidation states. Contrary to the experimental expectation, it is the orthogonal reactivity between $Ni^{I}(bpy)Br$ and $Pd^{0}(dppp)$ rather than that between $Ni^{0}(bpy)$ and $Pd^{0}(dppp)$ that can satisfy the need for such Ullmann cross-coupling reactions. Fig. 1 shows the Gibbs free energy changes (ΔG°) of coordinations and Gibbs activation energies ($\Delta G^{\circ\ddagger}$) of oxidative additions of **Ph-Br** and **Ar-OTf** to $Ni^{0}(bpy)$, $Ni^{I}(bpy)Br$ and $Pd^{0}(dppp)$, respectively. It can be seen that the coordinations of **Ph-Br** and **Ar-OTf** to $Ni^{0}(bpy)$ afford two corresponding pre-complexes with the ΔG° values of −25.0 and −27.1 kcal mol^{-1}, respectively. However, the $\Delta G^{\circ\ddagger}$ values of C–Br and C–OTf bond activations by $Ni^{0}(bpy)$ are 7.0 and 2.3 kcal mol^{-1}, respectively. These calculation results indicate that such a barrier-free coordination process is irreversible (Fig. S1 and S2, ESI†), so the thermodynamic stability of the pre-complex determines the substrate selectivity of $Ni^{0}(bpy)$. Specifically, $Ni^{0}(bpy)$ prefers to activate the C–OTf bond rather than the C–Br bond. By contrast, in the case of $Ni^{I}(bpy)Br$, the coordinations of **Ph-Br** and **Ar-OTf** are exothermic by only 6.0 and 13.2 kcal mol^{-1}, respectively. However, the oxidative additions of C–Br and C–OTf bonds to $Ni^{I}(bpy)Br$ need $\Delta G^{\circ\ddagger}$ values of 20.3 and 26.6 kcal mol^{-1}, respectively. Thus, the substrate selectivity of $Ni^{I}(bpy)Br$ depends on the activation barrier of oxidative addition. Compared to the C–OTf bond, $Ni^{I}(bpy)Br$ prefers to activate the C–Br bond to afford a reactive nickel(III) phenyl bromide intermediate $\mathbf{1}_{b}^{Ni}$ (Fig. S4, ESI†). In addition, $Pd^{0}(dppp)$ shows a chemoselectivity similar to $Ni^{0}(bpy)$. $Pd^{0}(dppp)$ prefers to activate the C–OTf bond rather than the C–Br bond,[12] because the coordination of **Ar-OTf** to $Pd^{0}(dppp)$ can afford a more stable pre-complex with a ΔG° value of −19.3 kcal mol^{-1}. Subsequently, a direct oxidative addition of the C–OTf bond to the palladium(0) center affords a relatively stable palladium(II) aryl triflate intermediate $\mathbf{1}_{a}^{Pd}$ with a $\Delta G^{\circ\ddagger}$ value of 12.0 kcal mol^{-1} (Fig. S5, ESI†).

In view of the necessity of $Pd^{0}(dppp)$ and $Ni^{I}(bpy)Br$ combination, the related calculations were carried out using the Dmol^3 code to evaluate the two successive single electron reduction process of $Pd^{II}(dppp)Cl_2$ and $Ni^{II}(bpy)Br_2$ on the Zn (101) surface, respectively (see the ESI† for methods). As shown in Fig. 2a, $Pd^{II}(dppp)Cl_2$ is more likely to be reduced to $Pd^{0}(dppp)$, which is more stable than $Pd^{I}(dppp)Cl$ by 60.8 kcal mol^{-1}. This result is consistent with a generally accepted cognition that a palladium complex shows double-electron performance.[13] As shown in Fig. 2b, however, the reduction of $Ni^{II}(bpy)Br_2$ to $Ni^{I}(bpy)Br$ is exergonic by −38.5 kcal mol^{-1}, whereas to $Ni^{0}(bpy)$ is endergonic by 11.3 kcal mol^{-1}. Thus, $Pd^{0}(dppp)$/$Ni^{I}(bpy)Br$ combination can be afforded favorably by the reducing agent (Zn).

After the selective oxidative additions, the subsequent aryl migration would proceed between the stable $\mathbf{1}_{a}^{Pd}$ and active $\mathbf{1}_{b}^{Ni}$, which is quite consistent with the persistent radical effect

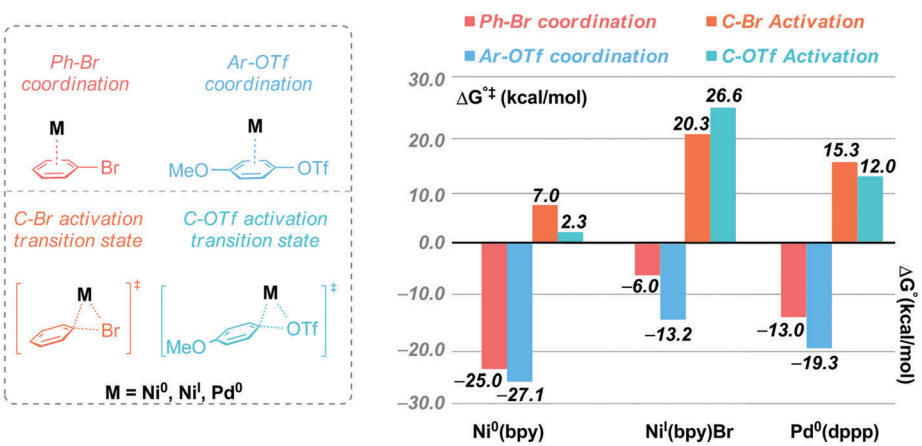

Fig. 1 Gibbs free energy changes (ΔG°) of the coordinations and Gibbs activation energies ($\Delta G^{\circ\ddagger}$) of the oxidative additions of **Ph-Br** and **Ar-OTf** to $Ni^{0}(bpy)$, $Ni^{I}(bpy)Br$ and $Pd^{0}(dppp)$, respectively.

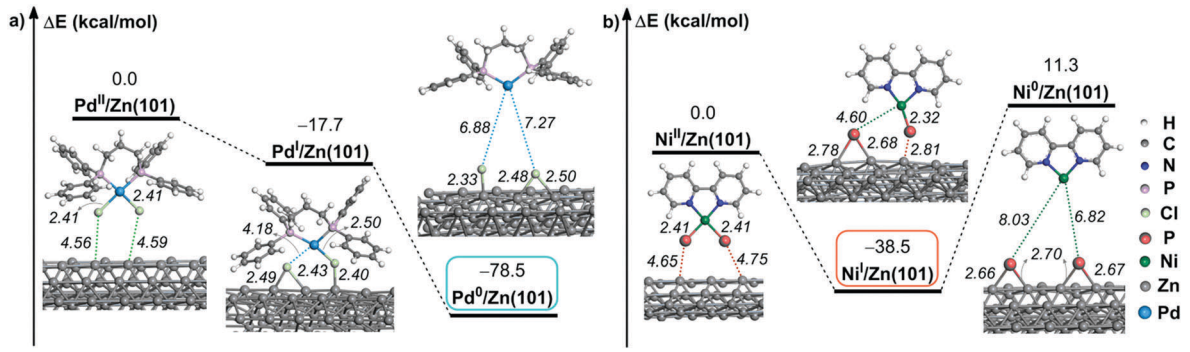

Fig. 2 Energy change (ΔE, kcal mol^{-1}) of the single electron reduction process of **Pd^{II}(dppp)Cl$_2$** and **Ni^{II}(bpy)Br$_2$** catalyzed by Zn dust. The bond distances are given in Angstroms.

accounted for the observed cross-selectivity experimentally.[6,14] Is the aryl group to be migrated to the Ni or Pd center? We have systematically investigated two reaction courses: a heterobimetallic transmetalation mechanism (Fig. 3) and a single electron radical transfer mechanism (Fig. S6, ESI†). As a result, the former is more favorable than the latter. In other words, the aryl group is more easily migrated to the Ni center to complete such Ullmann cross-coupling reactions. Specifically, in the heterobimetallic transmetalation mechanism, the aryl ring of $\mathbf{1}_a^{Pd}$ migrates to the Ni^{III} center of $\mathbf{1}_b^{Ni}$. A stable heterobimetallic dimer **2** is initially produced and is exergonic by 8.7 kcal mol^{-1}, in which Ni^{III} and Pd^{II} are bridged by a bromide ion. Subsequently, a direct transmetalation occurs *via* a four-membered Ni–C–Pd–Br ring transition state **TS2^{Ni}** to afford intermediate **3^{Ni}** with a $\Delta G^{\circ\ddagger}$ value of 19.5 kcal mol^{-1}. The dimeric **3^{Ni}** is dissociated into the palladium(II) bromide triflate **Pd^{II}(dppp)(Br)(OTf)** and diaryl nickel(III) intermediate **4^{Ni}** with a ΔG° value of −10.6 kcal mol^{-1}. Notice that **Pd^{II}(dppp)(Br)(OTf)** can be reduced to **Pd^{0}(dppp)** by Zn dust based on the above calculations. The following C–C coupling from **4^{Ni}** is nearly barrier-free, because the nickel(III) species readily facilitates the reductive elimination.[15] The desired cross-coupling product (**Ph-Ar**) and the **Ni^{I}(bpy)Br** catalyst were generated to complete the catalytic cycle with a ΔG° value of −35.8 kcal mol^{-1} relative to **4^{Ni}**. Alternatively, the phenyl migration from $\mathbf{1}_b^{Ni}$ onto the Pd center of $\mathbf{1}_a^{Pd}$ provides a Ni^{III}/Pd^{II} → Ni^{II}/Pd^{III} transformation because of the radical phenyl migration, which is named a single electron radical transfer mechanism (Fig. S6, ESI†). This step needs a larger $\Delta G^{\circ\ddagger}$ value of 24.1 kcal mol^{-1}. In addition, another possibility that the phenyl migration from Ni^{III} to Pd^{II} without alternation of the oxidation states has also been excluded (Fig. S7, ESI†). Accordingly, the most favorable full catalytic cycle of the present reaction consists of four key elementary steps: the oxidative addition of **Ar-OTf** to **Pd^{0}(dppp)** to afford the relatively stable $\mathbf{1}_a^{Pd}$, the oxidative addition of **Ph-Br** to **Ni^{I}(bpy)Br** to generate the reactive $\mathbf{1}_b^{Ni}$, the heterobimetallic Ni^{III}/Pd^{II} transmetalation to form **Pd^{II}(dppp)(Br)(OTf)** and **4^{Ni}**, and the reductive elimination to afford **Ph-Ar**, as shown in Scheme 2. The rate-determining step is the oxidative addition of **Ph-Br** to **Ni^{I}(bpy)Br** with a $\Delta G^{\circ\ddagger}$ value of 20.3 kcal mol^{-1}, which can be overcome under the experimental conditions (40 °C).[6] In this regard, it is in good accordance with the experimental observation that the increase of **Ni^{II}(bpy)Br$_2$** concentration rather than **Pd^{II}(dppp)Cl$_2$** can accelerate the cross-coupling reaction.[6] According to the above discussion, Ni plays a leading role in the present dual catalysis because of its participation in the entire reaction process.

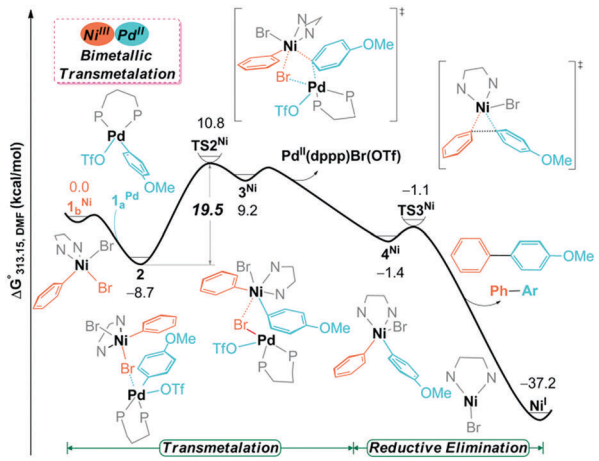

Fig. 3 The most favorable energy profiles ($\Delta G^{\circ}_{313.15}$) of the heterobimetallic transmetalation mechanism of Ni/Pd dual catalysis.

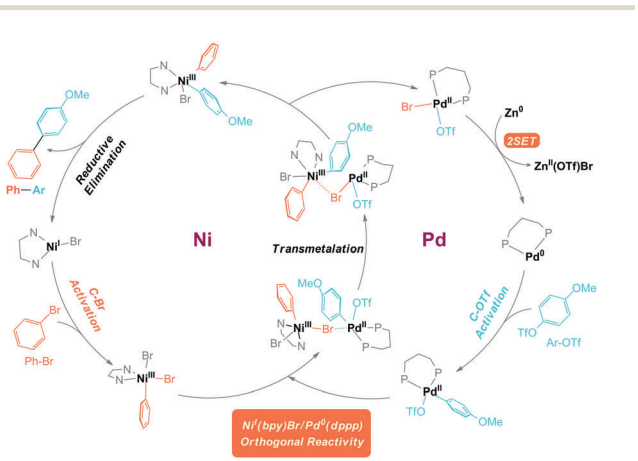

Scheme 2 The most favorable full catalytic cycle of the Ullmann C–C cross-coupling *via* Ni^{I}/Pd^{0} dual catalysis.

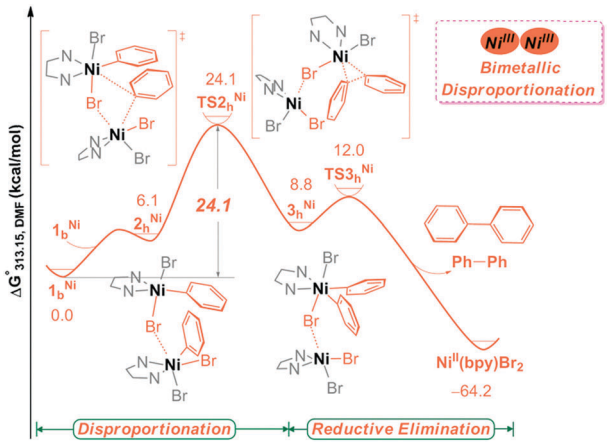

Fig. 4 Energy profiles ($\Delta G^{\circ}_{313.15}$) of the homobimetallic disproportionation mechanism of Ni catalysis.

In order to uncover the origin of cross-selectivity caused by **Ni^{I}(bpy)Br/Pd^{0}(dppp)** dual catalysis, we also studied the homo-coupling of **Ph-Br** catalyzed by **Ni^{I}(bpy)Br** independently (Fig. 4). As discussed above, the selective oxidative addition of the C–Br bond to **Ni^{I}(bpy)Br** occurs firstly to generate the transient $\mathbf{1_b^{Ni}}$ ($\Delta G^{\circ\ddagger}$ = 20.3 kcal mol^{-1}). Next, the radical phenyl migration between two nickel(III) intermediates $\mathbf{1_b^{Ni}}$ occurs through the phenyl scrambling transition state $\mathbf{TS2_h^{Ni}}$ to afford a mixed valence (Ni^{II}/Ni^{IV}) complex $\mathbf{3_h^{Ni}}$.[16] The $\Delta G^{\circ\ddagger}$ and ΔG° values for this Ni^{III}/Ni^{III} → Ni^{II}/Ni^{IV} disproportionation are 24.1 and 8.8 kcal mol^{-1}, respectively. Then, **Ph-Ph** reductive elimination occurs through the transition state $\mathbf{TS3_h^{Ni}}$ to form **Ni^{II}(bpy)Br$_2$**, which can be reduced to **Ni^{I}(bpy)Br** by Zn dust to restart the catalytic cycle. This reductive elimination needs a small $\Delta G^{\circ\ddagger}$ value (12.0 kcal mol^{-1} relative to $\mathbf{1_b^{Ni}}$). In addition, an alternative reductive elimination where **Ni^{II}(bpy)Br$_2$** is dissociated firstly from $\mathbf{3_h^{Ni}}$ needs a slightly larger $\Delta G^{\circ\ddagger}$ value of 13.0 kcal mol^{-1} (Fig. S8, ESI†). To sum up, the homo-coupling occurs *via* oxidative addition of the C–Br bond to **Ni^{I}(bpy)Br**, homobimetallic Ni^{III}/Ni^{III} disproportionation and C–C bond-forming reductive elimination to afford the homo-coupling product biphenyl (**Ph-Ph**) with the $\Delta G^{\circ\ddagger}$ value of 24.1 kcal mol^{-1}. Hence, the homo-coupling of **Ph-Br** catalyzed by **Ni^{I}(bpy)Br** is less favorable than the cross-coupling of **Ph-Br** and **Ar-OTf** *via* **Ni^{I}(bpy)Br/Pd^{0}(dppp)** dual catalysis ($\Delta G^{\circ\ddagger}$ = 20.3 kcal mol^{-1}), which shows the best consistency with the experimental observation (Scheme 1). Furthermore, the presence of **Pd^{0}(dppp)** is suggested to be responsible for the cross-selectivity of such Ullmann C–C cross-coupling, because the heterobimetallic Ni^{III}/Pd^{II} transmetalation is easier to occur than the homo-bimetallic Ni^{III}/Ni^{III} disproportionation.

In conclusion, the mechanistic details of the Ullmann C–C cross-coupling of bromobenzene and 4-methoxyphenyltriflate *via* Ni/Pd dual catalysis have been theoretically disclosed here. The orthogonal reactivity of Ni^{I}/Pd^{0} combination is the precondition and foundation of achieving such a reaction. The substrate selectivity of palladium(0) depends on the thermodynamic stability of the pre-complex, while the substrate selectivity of nickel(I) is determined by the activation barrier of oxidative addition. In the present dual catalysis, the Ni^{I} complex acts as the primary catalyst, while the Pd^{0} catalyst plays a decisive role in the cross-selectivity.

This work was financially supported by the NSFC (21773025, 21403033 and 61775212), the Fundamental Research Funds for the Central Universities, and the State Key Laboratory of Applied Optics. We acknowledge the National Supercomputing Center in Shenzhen for providing the computational resources.

Conflicts of interest

There are no conflicts to declare.

Notes and references

1 (*a*) Y. H. Sun, H. Tang, K. J. Chen, L. R. Hu, J. N. Yao, S. Shaik and H. Chen, *J. Am. Chem. Soc.*, 2016, **138**, 3715; (*b*) T. Bleith and L. H. Gade, *J. Am. Chem. Soc.*, 2016, **138**, 4972; (*c*) S. N. Kessler and J.-E. Bäckvall, *Angew. Chem., Int. Ed.*, 2016, **55**, 3734; (*d*) B. Sun, T. Yoshino, M. Kanai and S. Matsunaga, *Angew. Chem., Int. Ed.*, 2015, **54**, 13160; (*e*) S. Z. Tasker, E. A. Standley and T. F. Jamison, *Nature*, 2014, **509**, 299.
2 (*a*) J. Carey, D. Laffan, C. Thomson and M. Williams, *Org. Biomol. Chem.*, 2006, **4**, 2337; (*b*) J. Magano and J. R. Dunetz, *Chem. Rev.*, 2011, **111**, 2177; (*c*) S. D. Roughley and A. M. Jordan, *J. Med. Chem.*, 2011, **54**, 3451.
3 C. C. C. J. Seechurn, M. O. Kitching, T. J. Colacot and V. Snieckus, *Angew. Chem., Int. Ed.*, 2012, **51**, 5062.
4 (*a*) F. Ullmann and D. Bielecki, *J. Chem. Ber.*, 1901, **34**, 2174; (*b*) F. Ullmann, *Chem. Ber.*, 1903, **36**, 2382; (*c*) F. Ullmann and P. Sponagel, *Chem. Ber.*, 1905, **38**, 2211; (*d*) I. Goldberg, *Chem. Ber.*, 1906, **39**, 1691; (*e*) J. Hassan, M. Sévignon, C. Gozzi, E. Schulz and M. Lemaire, *Chem. Rev.*, 2002, **102**, 1359; (*f*) M. Amatore and C. Gosmini, *Angew. Chem., Int. Ed.*, 2008, **47**, 2089; (*g*) D. J. Weix, *Acc. Chem. Res.*, 2015, **48**, 1767; (*h*) T. Moragas, A. Correa and R. Martin, *Chem. – Eur. J.*, 2014, **20**, 8242.
5 C. E. I. Knappke, S. Grupe, D. Gartner, M. Corpet, C. Gosmini and A. J. von Wangelin, *Chem. – Eur. J.*, 2014, **20**, 6828.
6 L. K. G. Ackerman, M. M. Lovell and D. J. Weix, *Nature*, 2015, **524**, 454.
7 (*a*) K. N. Houk and F. Liu, *Acc. Chem. Res.*, 2017, **50**, 539; (*b*) B. Zhu, W. Guan, L. K. Yan and Z. M. Su, *J. Am. Chem. Soc.*, 2016, **138**, 11069; (*c*) W. Guan, S. Sakaki, T. Kurahashi and S. Matsubara, *ACS Catal.*, 2015, **5**, 1; (*d*) M. H. Larsen, K. N. Houk and A. S. K. Hashmi, *J. Am. Chem. Soc.*, 2015, **137**, 10668; (*e*) X. T. Qi, Y. Z. Li, R. P. Bai and Y. Lan, *Acc. Chem. Res.*, 2017, **50**, 2799; (*f*) X. H. Kang, G. Luo, L. Luo, S. W. Hu, Y. Luo and Z. M. Hou, *J. Am. Chem. Soc.*, 2016, **138**, 11550; (*g*) B. Zhu, L. K. Yan, Y. Geng, H. Ren, W. Guan and Z. M. Su, *Chem. Commun.*, 2018, **54**, 5968.
8 Y. Zhao and D. G. Truhlar, *Theor. Chem. Acc.*, 2008, **120**, 215.
9 M. Mammen, E. I. Shakhnovich, J. M. Deutch and G. M. Whitesides, *J. Org. Chem.*, 1998, **63**, 3821.
10 (*a*) V. Barone and M. Cossi, *J. Phys. Chem. A*, 1998, **102**, 1995; (*b*) M. Cossi, N. Rega, G. Scalmani and V. Barone, *J. Comput. Chem.*, 2003, **24**, 669; (*c*) J. Tomasi, B. Mennucci and R. Cammi, *Chem. Rev.*, 2005, **105**, 2999.
11 M. J. Frisch, *et al. Gaussian 09 (Rev. D.01)*, Gaussian, Inc., Wallingford, CT, 2013.
12 F. Schoenebeck and K. N. Houk, *J. Am. Chem. Soc.*, 2010, **132**, 2496.
13 G.-M. Max, A. C. Ataualpa, A. Braga, U. Gregori and M. Feliu, *Acc. Chem. Res.*, 2013, **46**, 2626.
14 (*a*) A. Studer, *Chem. – Eur. J.*, 2001, **7**, 1159; (*b*) H. Fische, *Chem. Rev.*, 2001, **101**, 3581.
15 J. A. Terrett, J. D. Cuthbertson, V. W. Shurtleff and D. W. C. MacMillan, *Nature*, 2015, **524**, 330.
16 J. B. Diccianni, C. H. Hu and T. N. Diao, *Angew. Chem., Int. Ed.*, 2017, **56**, 3635.

